Journal of The Electrochemical Society, **156** (1) P29-P37 (2009)
0013-4651/2008/156(1)/P29/9/$23.00 © The Electrochemical Society

Solid-State Electrochemistry in Molecule/TiO_2 Molecular Heterojunctions as the Basis of the TiO_2 "Memristor"

Jing Wu[a,b] and Richard L. McCreery[b,c,*,z]

[a]*Department of Chemistry, The Ohio State University, Columbus, Ohio 43210, USA*
[b]*National Institute for Nanotechnology, National Research Council, Alberta T6G 2G2, Canada*
[c]*Department of Chemistry, University of Alberta, Edmonton, Alberta T6G 2R3, Canada*

Thin-layer carbon/molecule/TiO_2/Au electronic junctions with 1.7–2.1 nm thick molecular layers exhibit voltage-induced conductance switching, which may be repeated for at least hundreds of read/set/read/erase cycles. A fluorene(Fl)/TiO_2 junction can be switched to a higher conductance "set" state by a positive voltage pulse and brought back to the lower conductance "erased" state by a negative pulse. Similar conductance changes occurred following exposure to H_2 or UV radiation, and the conductance change is completely inhibited in a dry atmosphere. The bias-induced conductance switching of TiO_2 junctions is consistent with electrochemical reduction of Ti^{IV} oxide to the much more conductive Ti^{III} oxide, analogous to a solid-state redox reaction. The observations are consistent with reduction of hydroxylated TiO_2 sites to a much more conductive Ti^{III} oxide by the electrons injected into the TiO_2 during a positive voltage pulse. If Fl is replaced by aminodecane ($C_{10}H_{21}N$) or nitroazobenzene, the conductance switching is modified slightly, consistent with TiO_2 being the active switching component. The results bear directly on the origin of the hysteresis observed in TiO_2-based junctions and also on their suitability as examples of recently reported "memristors" [J. J. Yang, M. D. Pickett, X. Li, D. Ohlberg, D. Stewart, and R. S. Williams, *Nat. Nanotechnol.*, **3**, 429 (2008)].
 [DOI: 10.1149/1.3021033]

Manuscript submitted July 10, 2008; revised manuscript received October 6, 2008. Published November 18, 2008.

The commercial importance of microelectronic memory components has driven a broad research effort into configurations that provide greater speed, lower volatility, higher density, or longer cycle life than current devices based on magnetic or charge storage.[1,2] The advent of molecular electronics has introduced memory devices based on changes in molecular conformation or redox state, including rotaxanes,[3-5] phenylethynyl compounds,[6,7] and nitroaromatic compounds.[8-10] Pronounced hysteresis in current/voltage curves is an important signature of memory devices and has been associated with a range of phenomena, including, among others, molecular redox events,[4,9,11] metal filament formation and destruction,[1,12-14] and doping of conducting polymers.[15-17] Several early molecular memory devices contained titanium as the initial metal layer on top of a molecular layer,[3,4,11,18-20] but it was recognized later that the titanium metal had in fact oxidized partially or completely to titanium oxides, including TiO_2.[9,21-24] We concluded in 2004 that, although there were spectroscopically observable changes in the redox state of nitroazobenzene/TiO_x memory devices, the dominant conductance change was due to bias-induced reduction of TiO_x from high resistivity TiO_2 to Ti^{III} or Ti^{II} oxide, which have conduction band electrons and much lower resistivity.[9,21,25] In approximately parallel developments, bias-induced conductance switching was reported in metal/metal oxide/metal devices containing TiO_2 or $SrTiO_3$, with the effects attributed to combinations of electron injection and ion motion in the TiO_2 lattice.[1,26-28] Thin films of TiO_2 exhibit various types of bias-induced switching behavior, both with and without additional molecules present, and several mechanisms underlying these changes have been reviewed recently.[1] Although there are some similarities in the current/voltage hysteresis and behavior of various memory devices that contain TiO_2, both the electronic response and underlying mechanism are strong functions of device fabrication and testing parameters.

The hysteretic current density-voltage (j-V) behavior reported for various TiO_2-containing memory devices was recently associated with a postulated circuit element dubbed a "memristor," for the case of Pt/TiO_2/TiO_{2-x}/Pt devices with an intentional layer of oxygen deficient TiO_2.[29,30] The existence and behavior of a memristor may have wide-ranging importance to circuit theory and design, including those involving embedded memory devices. Although the report by Yang et al.[29] proposed a mechanism based on transport of oxygen vacancies in TiO_2, there may also be redox processes and ion motion involved, and a detailed mechanism is unclear. Prior to the "memristor" reports, we continued our investigation of the mechanism of bias-induced conductance changes in TiO_2 by directly depositing TiO_2 from rutile onto a molecular layer by electron beam evaporation.[31] Carbon/fluorene/TiO_2/Au junctions exhibited robust, reversible conductance switching, with the junction conductance increasing by several orders of magnitude after the Au electrode was biased negative. Replacing the TiO_2 with a nonredox active oxide (Al_2O_3) completely eliminated conductance switching. We proposed a mechanism based on the fluorene layer acting as a tunneling barrier, such that a negative shift occurs in the Fermi level of TiO_2 when Au was biased negative, resulting in reduction of TiO_2 to the more conductive Ti^{III} oxide.[31] This TiO_2 reduction process amounts to dynamic doping of TiO_2 by electron injection from the imposed electric field.

In our previous investigation,[31] we noted the sensitivity of junction structure to the ambient atmosphere, but did not explore it in detail. We subsequently determined that atmosphere, notably humidity and oxygen content, plays an important role in the mechanism of bias-induced conductance changes in TiO_2. The current work was undertaken to understand chemical factors affecting conductance switching of molecule/TiO_2 heterojunctions and their bearing on the conductance switching mechanism. Nitroazobenzene, fluorine, and aminodecane were compared as molecular layers, and the oxides included TiO_2, SiO_2, and Al_2O_3. Oxygen vacancies and hydration in the TiO_2 were manipulated during and after junction fabrication, in order to elucidate the conductance switching mechanism responsible for the behavior of molecule/TiO_2 devices. The results are interpreted in terms of their relevance to the broad range of TiO_2 memory devices, including the Pt/TiO_2/Pt memristor.

Experimental

Molecular junctions of the "cross-junction" configuration were fabricated on a thermally grown silicon dioxide surface as described in detail previously.[32-34] Briefly, a 0.5 mm wide strip of oxide and Au was deposited perpendicular to a 0.5 mm strip of pyrolyzed photoresist film (PPF) previously modified with molecular layers to form a junction 0.0025 cm^2 in area. PPF is similar to glassy carbon in structure, with <0.5 nm surface roughness and a resistivity of 0.006 Ω cm.[35,36] Ten nanometers of TiO_2 was deposited in an electron-beam evaporator (Kurt J. Lesker PVD75) at a rate of 0.02 nm/s. Rutile was used as the target, and the pressures of O_2 and H_2O were controlled in a range of $(2–4) \times 10^{-5}$ and $(0.5–1) \times 10^{-5}$ Torr, respectively, during deposition as measured by a re-

* Electrochemical Society Fellow.
z E-mail: richard.mccreery@ualberta.ca

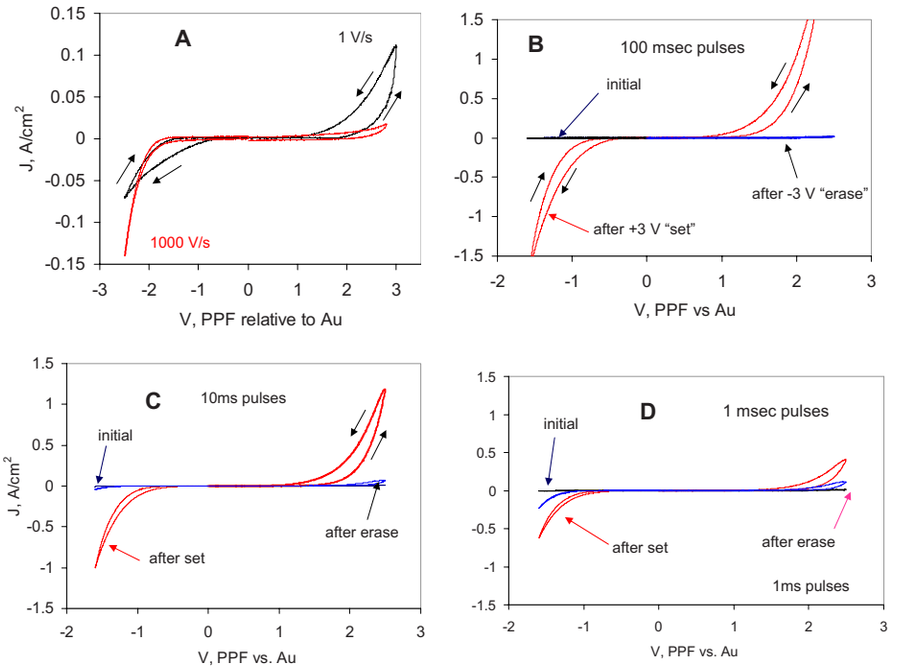

Figure 1. (Color online) Hysteresis and bias-induced conductance switching of PPF/Fl/TiO_2/Au junctions prepared with controlled deposition atmosphere. (A) Initial scans at 1 V/s (dark curve) and 1000 V/s (gray curve) starting at 0 V in a + direction (PPF relative to Au). Arrows indicated scan direction. (B) 1000 V/s scans initiated at 0 V in a + direction before ("initial") and immediately after a +3 V, 100 m "set" pulse and a −3 V, 100 ms erase pulse, in that order. (C, D) are the same as (B), but for 10 and 1 ms set and erase pulses, respectively. All *j-V* scans and pulses were acquired in three-wire mode, in ambient air.

sidual gas analyzer (Stanford Research Systems RGA/200). Au was deposited through the same shadow mask as TiO_2 at a rate of 0.02 nm/s, and O_2 and H_2O pressures were controlled to be (3–5) × 10^{-6} and (1–2) × 10^{-6} Torr, respectively, during Au deposition. Al_2O_3 and SiO_2 were deposited under the same conditions as TiO_2. In all cases reported below, 10 nm oxide and 15 nm Au layers were used as determined with a quartz crystal microbalance during deposition and verified by atomic force microscopy (AFM).[31] Several PPF/Fl/TiO_2/Pt junctions were prepared with 15 nm of Pt instead of Au, and they behaved similarly to Au junctions, including their response to H_2 and UV light. Fluorene (Fl) and nitroazobenzene (NAB) were deposited on PPF from their diazonium ion precursors[37] and aminodecane by oxidation of 1-amino-n-decane.[38] Molecular layer thicknesses for Fl and NAB were determined to be 1.7 and 1.9 nm by AFM "scratching" as reported previously.[37] The $C_{10}N$ layer thickness was measured as 2.1 ± 0.3 nm using the same AFM method.

Electronic properties of junctions were characterized in a three wire configuration described previously,[32] in which ohmic voltage losses in the PPF lead were corrected. Controlled atmosphere experiments were performed in a cryogenic probe station (Janis Research ST 500), which was turbo pumped to a base pressure of ~5 × 10^{-6} Torr. During controlled atmosphere experiments, the sample chamber was refilled with desired gas back to ~1 atm after initial evacuation. All voltages are stated as PPF relative to Au, and positive current indicates electron flow from the Au through the junction to PPF. Junction sealing was conducted by attaching a piece of cover glass onto junctions with epoxy (LePage 5-Minute Epoxy). Controlled humidity was produced in a desiccator containing water/glycol mixtures and measured by a humidity and temperature recorder (Barnstead RHTEMP101). Ambient humidity varied between ~25 and 50% during the several month period when junctions were tested in lab air.

Results

We previously reported hysteresis and conductance switching in a Fl/TiO_2 heterojunction, with a high conductance state following a +3 V set pulse and a low conductance state after a −3 V erase pulse.[31] In the course of changing laboratories and installing an E-beam evaporation system, we noted that junction behavior was a strong function of the atmosphere during TiO_2 evaporation and after removal from the vacuum chamber. In particular, variations in water and O_2 levels during and after deposition had major consequences for junction conductance and switching. Accordingly, these variables were controlled and monitored with a residual gas analyzer during TiO_2 and Au deposition, and conditions were determined that produced reproducible junction behavior. To assess junction reproducibility, 10 PPF/Fl/TiO_2/Au junctions were prepared with controlled O_2 (2–4 × 10^{-5} Torr) and H_2O (0.5–1 × 10^{-5} Torr) pressures during TiO_2 deposition, and characterized electronically in air within 1 h after fabrication. For initial current *j-V* curves obtained at a scan rate of 1000 V/s, the voltage (mean ± standard deviation) at which the current density reached +0.05 A/cm^2 was 1.65 ± 0.11 V, while it reached −0.05 A/cm^2 at −1.25 ± 0.05 V for negative bias. Figure 1A shows *j-V* curves for a PPF/FL/TiO2/Au junction made with controlled H_2O and O_2 levels at two voltage scan rates. A 1 V/s slow scan shows pronounced hysteresis, very similar to that reported previously,[31] while the hysteresis is absent for the 1000 V/s scan. As described in previous papers,[11,31] we have found a pulse and scan paradigm more useful than a single *j-V* curve for investigating memory effects, in which fast 1000 V/s scans are acquired before and after set and erase voltage pulses. The 1000 V/s scans are fast enough to minimally perturb the junctions, and provide a snapshot of the *j-V* behavior following various voltage pulses. Figure 1B shows a "memory cycle" of fast scans acquired before (initial), after a +3 V, 100 ms set pulse, and again after a −3 V, 100 ms erase pulse. As reported previously,[31] the set pulse shape shows a smooth increase in current with time after application of the +3 V bias, as expected from Fig. 1A. Figures 1C and D show the effect of decreasing the pulse durations to 10 and 1 ms, respectively. Figure 1C shows qualitatively similar behavior to that reported previously for 100 ms pulses,[31] with a +3 V set pulse generating a large increase in conductance and a −3 V erase pulse causing a conductance decrease. As apparent in Fig. 1D, the set conductance is smaller for the shorter, 1 ms pulses, and the erase is incomplete for a 1 ms, −3 V pulse. We found that the erase process is more complete when the erase pulse is significantly longer than the set pulse, with a 1 ms, +3 V set and 50 ms, −3 V erase pulse producing a good contrast between the set and erased *j-V* curves.

The set dynamics are shown as a function of pulse voltage and

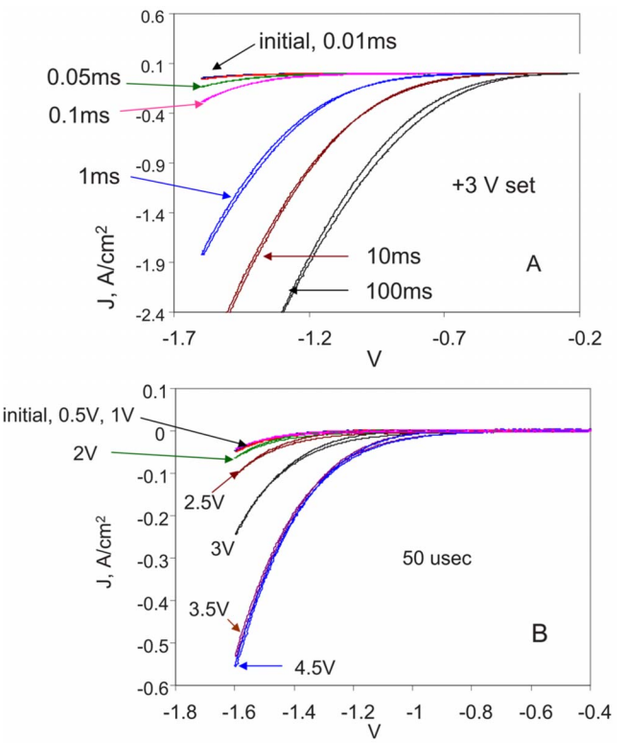

Figure 2. (Color online) "Set" state conductance after a series of set pulses. (A) 1000 V/s scans acquired before and after 0.01, 0.05, 0.1, 1, 10 and 100 ms +3V pulse. (B) 1000 V/s scans acquired before and after 50 μs set pulse ranging from +0.5 to +4.5 V. Junctions were erased and allowed to stand for >2 h between set pulses.

pulse length in Fig. 2. We noted that even a 1000 V/s positive scan could partially set the junction; thus, only negative scans were used to elucidate the relationship between set state conductance and pulse conditions, and the junction was erased and allowed to rest for >2 h between set pulses. Figure 2a shows *j-V* curves of the initial state, and after a series of +3V set pulses lasting from 10 μs (the lower limit of the instrument), to 100 ms. The set state conductance increases monotonically with pulse length in the range studied, and pulses longer than 100 ms often caused irreversible junction damage. Figure 2b shows *j-V* curves following 50 μs set pulses of increasing voltage, from 0.5 to 4.5 V. The junction shows negligible change after a 50 μs set pulse lower than 2 V, but the set state conductance increases with set pulse voltage above 2 V until it reaches a maximum at +3.5 V. To minimize junction damage caused by high currents, many of the results reported henceforth were obtained with 1 ms, +3 V set, and 50 ms, −3 V erase pulses. A read/set/erase memory cycle using these conditions is shown in Fig. 3A.

We next observed the effect of postdeposition atmosphere on device behavior by exposing completed junctions to various conditions after removal from the electron beam chamber. Figure 3A was obtained in ambient air, then the same junction was exposed to vacuum ($\sim 5 \times 10^{-6}$ Torr) for 12 h, and the memory cycle of Fig. 3B was obtained using otherwise identical conditions. Vacuum exposure nearly completely eliminated the conductance increase caused by a +3 V set pulse. Furthermore, the large increase in conductance observed during a 100 ms, +2.2 V pulse shown in Fig. 3C was completely eliminated in a vacuum. We previously attributed this increase in conductance during a set pulse to reduction of TiO_2 to Ti^{III} oxide,[31] and Fig. 3D demonstrates that the conductance change is dependent on an atmospheric component. Introduction of dry oxygen did not restore switching, but exposure to water did, as shown in Fig. 4, obtained for the same junction after return to air of varying humidity. As shown in Fig. 4A, 3% relative humidity had little effect, while 24% nearly completely restored the switching observed before exposure to vacuum (Fig. 4B). Humidity of >50% was deleterious to switching (e.g., 60% for Fig. 4C), with *j-V* curves similar to those observed in 3% humidity. As apparent in the initial scans for the various humidity conditions (Fig. 4D), the apparent capacitance of the junction increased with humidity, with the 24% curve close to that observed before exposure to vacuum. It should be noted from panel Fig. 4B that the junction may be set merely by scanning to positive voltage without a set pulse, because the bias is above the ~2.5 V switching threshold for ~1 ms during the positive scan.

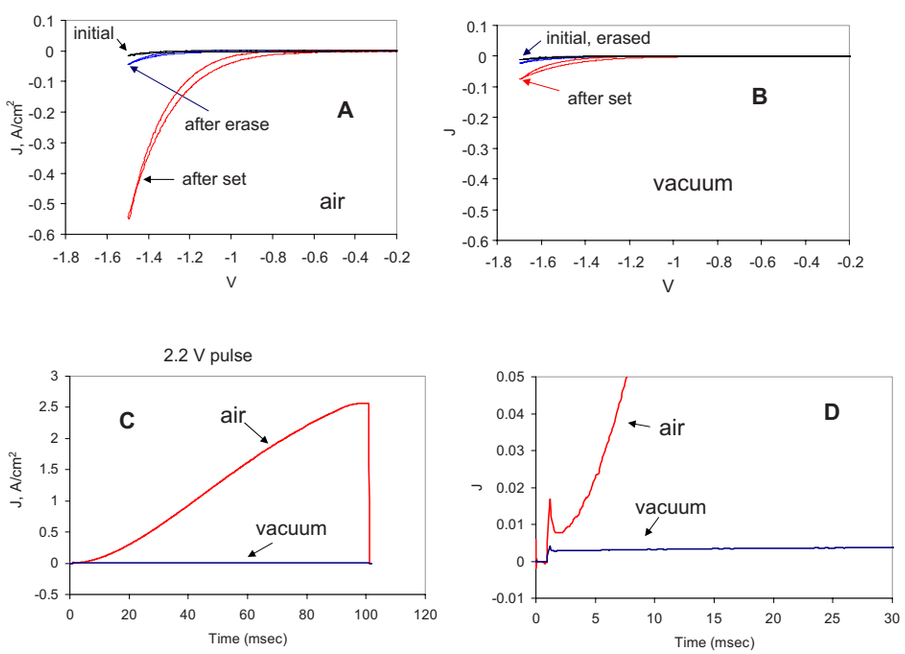

Figure 3. (Color online) Conductance switching of Fl/TiO_2 junctions in air and vacuum: 1 ms, 3 V set pulse, 50 ms, −3 V erase pulse, scan rate 1000 V/s. (A) air and (B) same junction after exposure to vacuum for ~12 h. (C) is the response to a +2.2 V, 100 ms pulse in air and in vacuum, and (D) is the same data on an expanded scale.

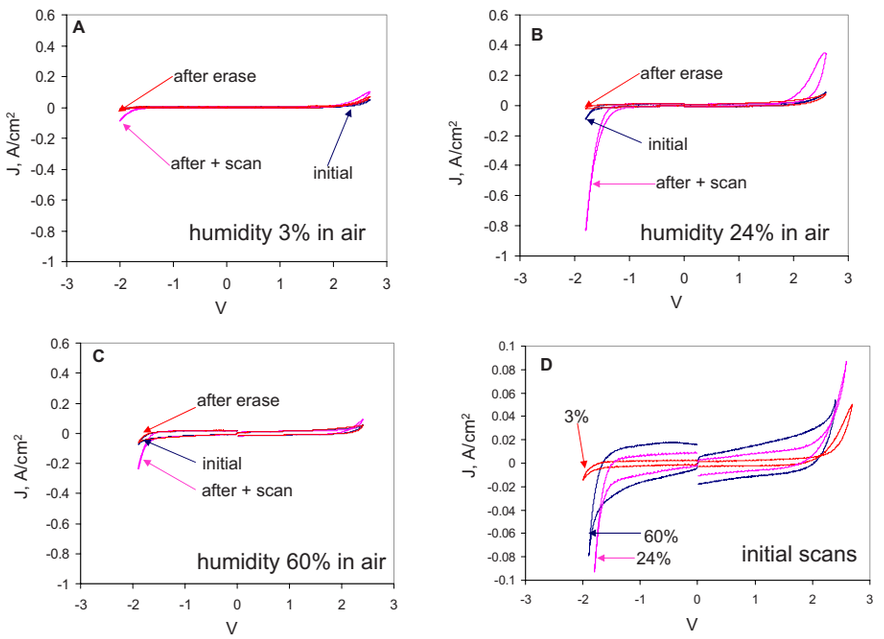

Figure 4. (Color online) Conductance switching of Fl/TiO_2 junctions in air of varying humidity after vacuum exposure. Erase pulse was −3 V, 50 ms, and junctions were set by a 1000 V/s scan to +2.7 V. (A) Initial 1000 V/s scans acquired in 3, 24, and 60% humidity, (B) in 3% humidity, (C) in 24% humidity, and (D) in 60% humidity.

To verify the role of TiO_2 in conductance switching, we substituted SiO_2 and Al_2O_3 for the TiO_2 in Fl/TiO_2 junctions. As shown in Fig. 5B and C, substitution of TiO_2 with SiO_2 or Al_2O_3 of equal thickness completely eliminates switching behavior, and results in permanently insulating junctions. Figure 6 shows the overlays of initial *j-V* curves of Fl junctions with different oxides in air and vacuum ($\sim 5 \times 10^{-6}$ Torr). All three types of junctions acted as capacitors at low voltage, with a constant current observed for a given scan rate expected for a parallel plate capacitor. The apparent dielectric constants of the junctions were calculated from the capacitive current, assuming a junction thickness of 12 nm. The apparent dielectric constants decreased when the junctions were exposed to vacuum for all three oxides and equaled 4.2 (Fl/SiO_2), 5.2 (Fl/Al_2O_3), and 10.5 (Fl/TiO_2) in vacuum. For a bias magnitude above ~1.5 V, the current across the Fl/TiO_2 junction increased dramatically, indicating electron injection into the TiO_2 conduction band, whereas Al_2O_3 and SiO_2 always block electron transfer in the voltage range studied.

Although we proposed previously[31] that H_2O may be involved in a bias induced redox reaction of TiO_2, the current results show that H_2O is a requirement for conductance switching in Fl/TiO_2 junctions. In order to elucidate further the importance of TiO_2 reduction to conductance switching, chemical and photo-induced TiO_2 reduction were investigated and compared to the effects of a voltage bias. The initial *j-V* curve in Fig. 7A was obtained from a Fl/TiO_2 junction exposed to vacuum for >1 h. Then, the sample chamber was filled with 5% H_2/N_2 gas for ~12 h, resulting in a *j-V* curve with

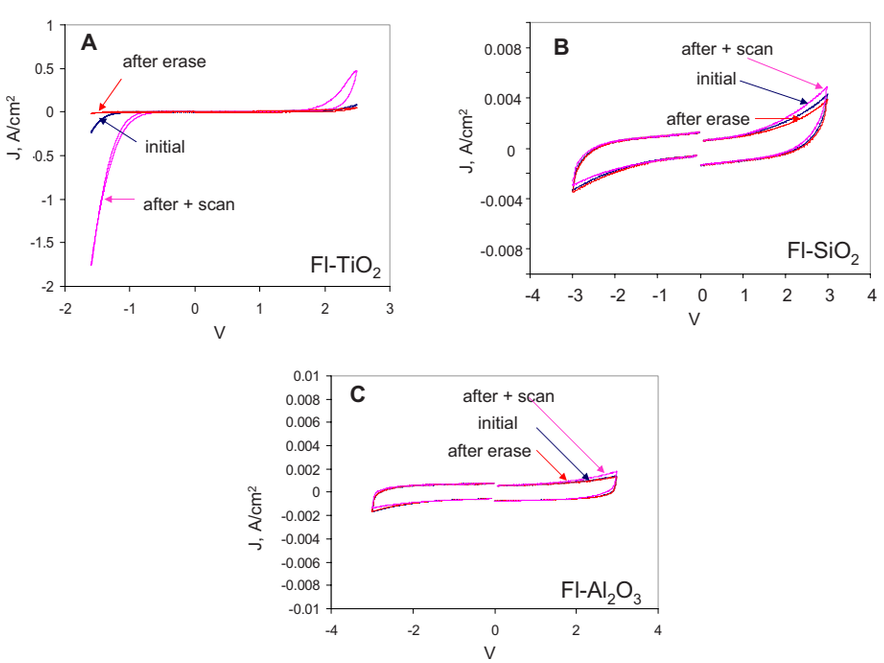

Figure 5. (Color online) Comparison of *j-V* curves for PPF/Fl/oxide/Au junctions using the same conditions as Fig. 4: (A) PPF/Fl/TiO_2/Au, (B) PPF/Fl/SiO_2/Au, and (C) PPF/Fl/Al_2O_3/Au.

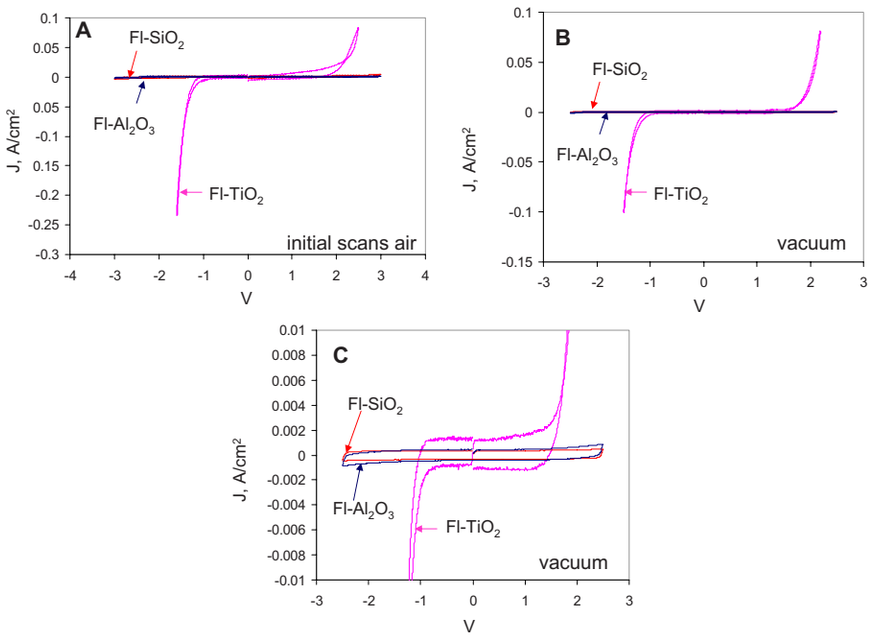

Figure 6. (Color online) Overlays of initial *j-V* curves for Fl/TiO_2, Fl/SiO_2, and Fl/Al_2O_3 junctions in air and vacuum, using the conditions of Fig. 4: (A) in air, (B) after >2 h in vacuum, (C) same as (B), but with magnified current density axis.

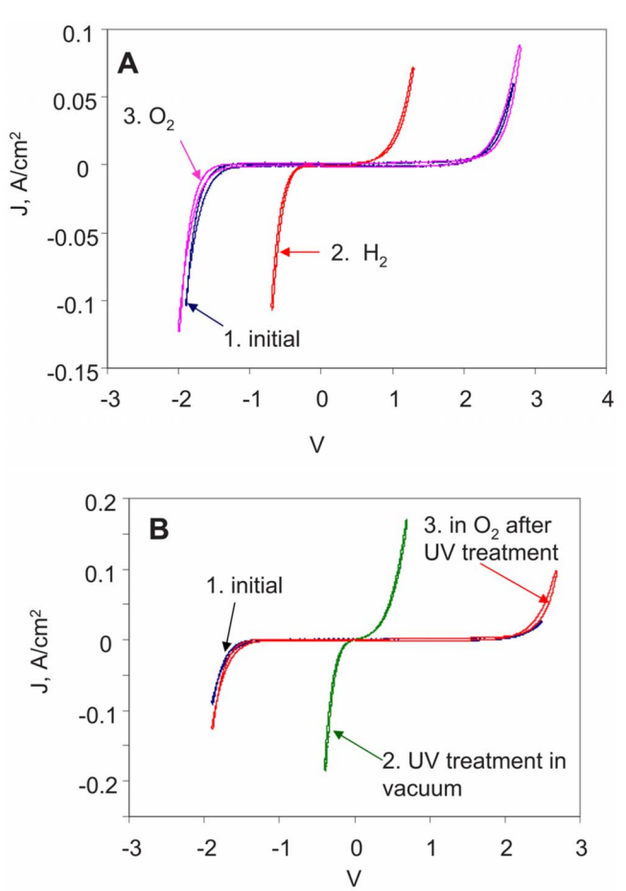

Figure 7. (Color online) H_2 and UV-induced conductance changes in a Fl/TiO_2 junction. *j-V* curves obtained at 1000 V/s, without intervening pulses. (A) 1. Initial, after >1 h in vacuum; 2. after exposure to 5% H_2/N_2 for >2 h; 3. After ~1 atm O_2 for 2 h. (B) Effect of UV exposure in vacuum and O_2, as indicated.

much higher conductance. Upon replacing the H_2/N_2 atmosphere with O_2, the junction conductance decayed back to the initial state in ~2 h. Exposure of the junction to UV light also changed junction conductance, as shown in Fig. 7B. The initial *j-V* curve was obtained in a vacuum then the junction was exposed to a UV "black light" (UVG-11 with 4 W mercury vapor tube, Thomas Scientific). UV light caused a large increase in junction conductance which persisted in vacuum until exposure to O_2 restored the conductance to that observed before UV exposure. Without oxygen, the UV-treated junction conductance decayed quite slowly, requiring more than 15 h in vacuum to relax to the initial state. The results of Fig. 7 establish that chemical reduction and oxidation with H_2 and O_2, and photoreduction with UV light produce conductance changes in the Fl/TiO_2, which are qualitatively similar to those induced by an applied bias, in both direction and reversibility. It should be noted that the bias-induced changes occurred with millisecond and submillisecond pulses, while conductance changes induced by H_2 and O_2 were much slower, requiring many minutes.

In order to reduce the atmospheric effects on Fl/TiO_2 junctions, samples were sealed with a small section of a glass microscope slide (~1 × 1 mm) attached directly on top of the junction with epoxy. Figure 8A shows the effects of humidity on the conductance change following a "set" pulse for an unsealed junction and is consistent with the results shown in Fig. 4A and B. When a junction was sealed in ~24% air, then exposed to varying humidity, the effect of humidity changes on conductance was negligible (Fig. 8B). The glass/epoxy seal was less effective for blocking changes induced by H_2 and O_2, presumably due to their small size and low polarity permitting permeation through epoxy and glass. As shown already in Fig. 7A, an unsealed junction treated with H_2 was completely restored to its initial state by 2 h of O_2 exposure. The sealed junction also showed a conductance increase with H_2 exposure (Fig. 8C), but the return to low conductance in O_2 was much slower, requiring at least 44 h to reach its low conductance state. Sealing is also beneficial to the retention of the high-conductance state of a Fl/TiO_2 junction after a set pulse. The current at −1.4 V decayed by 69% within 1 min after a 3 V set pulse, and returned to its initial value after 11 min. The current at −1.4 V for a sealed junction decayed 40% within 1 min after the set pulse and was still twice as large as the value preceding the set pulse after 11 min. Similarly, the UV-

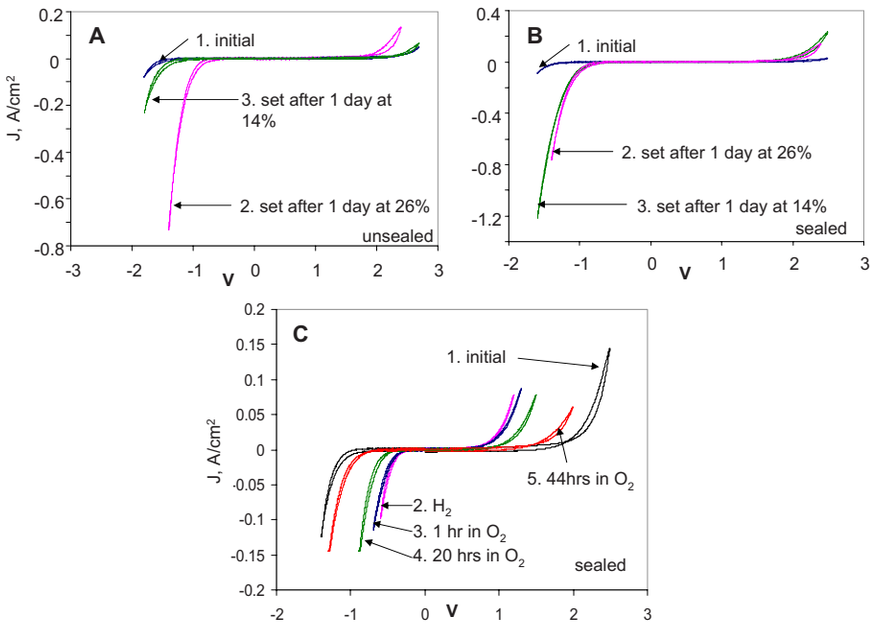

Figure 8. (Color online) Behavior of sealed and unsealed PPF/Fl/TiO_2/Au junctions with changes in atmosphere, in the order indicated. A single device was used for each panel. (A) unsealed, 1. Initial (same curves for 14 and 26% humidity); 2. After a set pulse for a junction exposed to 26% humidity for 1 day; 3. After set pulse for same junction after exposure to 14% humidity for 1 day. (B) Same sequence as (A), but with a sealed junction. (C) Sealed junction, initial, after ~12 hrs in H_2/N_2 (1 atm), and after 2 hours in 1 atm O_2. (D) 1. Initial, in air; 2. After ~12 h in 5% H_2/N_2 (1 atm); 3–5, after 1, 20, and 44 h in 1 atm O_2, respectively.

induced conductance increase is also sensitive to air and O_2, with a junction in air showing very little conductance increase upon UV exposure.

The memory cycle shown in Fig. 3A could be repeated for at least tens of cycles for a given junction. The repetitions were indistinguishable from the initial cycle provided the period between repetitions was long (i.e., >2 h). Longer endurance was evaluated by repetitive set/erase cycles consisting of 1 ms set pulses and 50 ms erase pulses, repeated every 10 min. As shown in Fig. 9, the magnitudes of the currents decreased gradually with repeated memory cycles, with the set current at −1.5 V decreasing by 20% after 66 cycles and 75% after 456 cycles. However, this decrease was reversed if the junction was left at open circuit in air for two days, indicating that the current decline did not result from irreversible chemical changes.

To consider the effects of molecular structure on conductance switching, PPF/molecule/TiO_2/Au junctions were prepared with NAB or $C_{10}H_{21}NH$ ($C_{10}N$) layers in place of fluorene, with all three molecular layers having measured thicknesses (by AFM) between 1.7 and 2.1 nm. All conditions of deposition, atmosphere, and electronic testing were kept constant, with the exception of the PPF surface modification. Figure 10 compares memory cycles of Fl/TiO_2, NAB/TiO_2, and $C_{10}N/TiO_2$ junctions in air with 26% humidity and all other conditions identical. Unlike the major changes noted in Fig. 5A when the oxide composition is changed, different molecular layers had relatively minor effects on conductance switching. All three cases showed a reversible increase in conductance following a +3 V set pulse, and all three were erased by a −3 V pulse. Fl/TiO_2 and $C_{10}N/TiO_2$ often showed higher conduc-

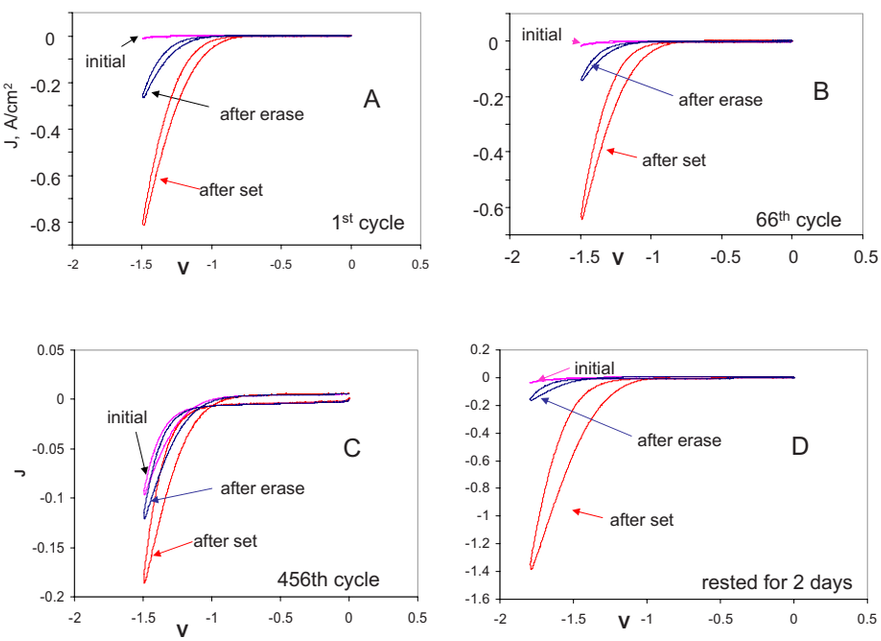

Figure 9. (Color online) *j-V* curves (1000 V/s) from a glass/epoxy sealed Fl/TiO_2 junction obtained at various points in a series of memory cycles consisting of +3 V, 1 ms set and −3 V, 50 ms erase pulses, repeated at 10 min intervals. A. Initial, after set pulse, and after erase pulse for first cycle; (B) 66th cycle; (C) 456th cycle; (D) two days at rest after the 456th cycle.

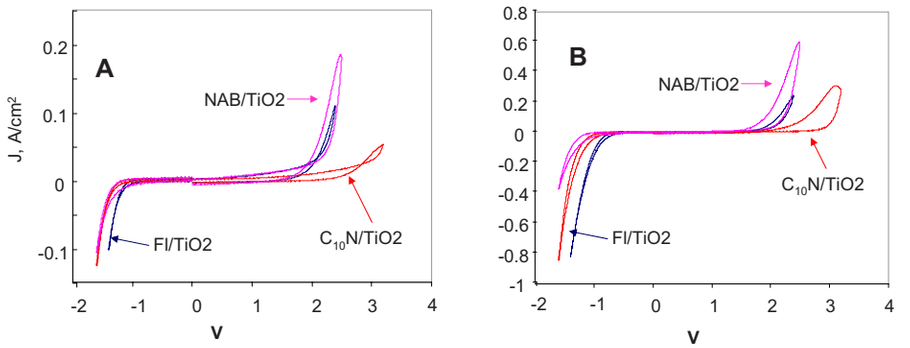

Figure 10. (Color online) Conductance switching of different molecule/TiO_2 junctions. (A) Initial 1000 V/s scans of Fl, NAB, and $C_{10}N$ TiO_2 junctions. (B) *j-V* curves of the same junctions after a 1000 V/s set scan to +2.4 V (Fl), +2.5 V (NAB), and +3 V ($C_{10}N$).

tance after a set pulse than NAB/TiO_2, although the difference was not dramatic. The rectification reported previously for NAB/TiO_2 junctions was less pronounced for the 1.9 nm thick NAB layer compared to the 4.5 nm layer used previously.[32]

Discussion

We previously used Raman spectroscopy to conclude that NAB can be reduced in a PPF/NAB/oxide/Au junction by a negative bias applied to the PPF contact.[9,33] The observation that molecule/TiO_2 junctions containing the redox inactive molecular layers fluorene and $C_{10}N$ also exhibit conductance switching confirms the conclusion that the switching can occur without known structural changes in the molecule accompanying redox activity. Furthermore, substituting a redox inactive oxide (SiO_2 or Al_2O_3) completely eliminates conductance switching, even though previous experiments showed that NAB still undergoes reduction if a bias is applied to a PPF/NAB/Al_2O_3/Au junction.[33] These results all confirm the conclusion that TiO_2 is the active agent for the observed switching behavior, rather than the molecular layer. Although NAB can be reduced in a NAB/Al_2O_3 junction, the overall conductance is controlled by the insulating oxide layer, which is presumably unchanged by the applied bias. As noted previously, partially reduced TiO_2 is expected to have a conductivity many orders of magnitude higher than Ti^{IV} oxide, due to the creation of conduction band electrons upon reduction.[9,31]

The similarity between a Fl/TiO_2 junction set by a positive pulse and one chemically reduced by H_2 or photoreduced by UV light support the conclusion that the applied bias causes electrochemical reduction of the TiO_2 during the set procedure. As noted above, the bias-induced reduction is much faster than that caused by H_2, with at least part of the difference attributable to mass transport of H_2 into the junction interior. The most likely route for H_2 entry into the junction is through a partially porous Au layer visible in scanning electron microscopy images (not shown) of the completed junction. As noted regarding Fig. 7, the conductance increase induced by H_2 or UV light is completely reversed by exposure to O_2. The absence of conductance switching when water is excluded implies that the reduction reactions are dependent either on water itself or on an ion derived from water (i.e., H^+ or OH^-). We proposed Reaction 1 as a possible reduction mechanism previously,[31] but Reaction 2 is another possibility

$$2TiO_2 + H_2O + 2e^- \rightarrow Ti_2O_3 + 2OH^- \quad [1]$$

$$TiO_2 + H_3O^+ + e^- \rightarrow TiO(OH) + H_2O \quad [2]$$

For the case of photoreduction by UV light, a useful precedent is provided by Szczepankiewicz et al.,[39,40] who monitored the photoreduction of TiO_2 with infrared spectroscopy and proposed that the dominant reaction is between hydrated Ti^{IV} sites and photogenerated conduction band electrons, as shown in Reaction 3

$$e^- + Ti^{IV}O\text{–}H \rightarrow Ti^{III}O\text{–}H^- \quad [3]$$

Reactions 1-3 share the common properties of producing Ti^{III} with its mobile d-band electrons, requiring water, and involving a reaction between conduction band electrons and Ti^{IV} sites. Because the TiO_2 is polycrystalline and disordered, it is difficult to be more precise about specific lattice sites, including the role of possible oxygen vacancies or small amounts of mobile ions from water or impurities. The proposal[29,30] of bias induced drift of positively charged oxygen vacancies in the memristor is not fundamentally different from reduction of Ti^{IV} to Ti^{III} with accompanying motion of O^{2-} ions. Because O^{2-} is energetically difficult to form, particularly at room temperature, it is more likely that ions derived from water are the mobile species, notably OH^-.

Szczepankiewicz et al.[39,40] also proposed a kinetic model for photoreduction of hydrated Ti^{IV} to Ti^{III}, which stated that the rate of generation of Ti^{III} is proportional to the concentration of hydrated Ti^{IV} times the concentration of conduction band electrons $[e^-_{cb}]$. For the bias induced reduction studied here, $[e^-_{cb}]$ is the space charge of electrons injected from Au into the TiO_2. This space charge will be larger for higher positive bias, and the hydrated Ti^{IV} concentration is higher in higher humidity. This model is consistent with the current observation of more rapid and larger conductance increases at more positive bias and higher humidity, up to a limit. Henderson[41] reported that the first several layers of water absorbed onto TiO_2 reacted with the surface much more strongly than water-water interactions in a multilayer, and the initial water layer contributes to TiO_2 hydration. After the initial water layers are adsorbed, more water did not increase TiO_2 hydration and depleted conduction band electrons.[42] The continued increase in capacitance and low voltage conductance with humidity shown in Fig. 4D implies that another charge transport mechanism may be operative at high water content, such as ionic conduction of protons or other small ions in a "damp" junction. The fact that high water content is deleterious to conductance switching implies that ion motion is not in itself sufficient to explain the observed conductance changes. However, it is still possible that ion motion accompanying hydration, such as H^+ transport between water molecules, may play a role in controlling local electric fields and in compensating space charge generated by electron injection and Ti^{IV} reduction.

If TiO_2 hydration was kept constant by controlling humidity at a moderate level of ~26%, the set state conductance became a function of set pulse voltage and length, as shown in Fig. 2. At voltages of >2 V, electrons inject into the TiO_2 conduction band and the set state conductance starts to increase as a result of electron trapping and formation of Ti^{III}. When the bias is >3.5 V, the set state conductance reaches a maximum. The asymptotic approach of the conductance to a maximum value with time after set pulse initiation is expected for a kinetic model involving reduction of a finite number of hydrated Ti^{IV} sites by injected electrons, and represents a combination of the kinetics of electron injection into the conduction band and the reduction reaction of Eq. 1 and 2.

Although the bias-induced changes are much faster than those from H_2 or O_2, the electronic "erase" process is significantly slower than the set. For entropic reasons, at least, it should be easier to inject electrons from a metal than to remove them from a low density of Ti^{III} sites in the oxide. The gradual loss of contrast between the "on" and erased states after hundreds of set/erase cycles shown in Fig. 9 is likely a result of incomplete oxidation of Ti^{III} by the erase pulses. It is likely that the generation of Ti^{III} occurs mainly at the Au/TiO_2 interface, followed by relatively slow migration of Ti^{III} sites into the oxide film by redox exchange or migration of oxygen vacancies. Repetitive cycling may eventually lead to a disordered distribution of Ti^{III} sites in the oxide, which are slowly oxidized by O_2 during a "rest" period. A related possibility is the formation of conducting tracks or filaments of Ti^{III} sites during the set pulse, which then dissipate slowly into the oxide.

The memristor based on $Pt/TiO_2/Pt$ junctions was postulated to function by motion of oxygen vacancies as "dopants" in TiO_2, with the distribution of vacancies resulting in changes in the relative magnitude of two series resistors.[29,30] Both here and in several past reports, we have discussed doping of TiO_2 in terms of reduction of Ti^{IV} to Ti^{III}, with accompanying large increase in conductivity.[9,21,31,32] Ti^{IV} reduction is equivalent to forming oxygen vacancies, although there may be a transient space charge following electron injection into TiO_2. We maintain that while ion motion may be involved in the conductance switching phenomenon, the process is in fact a solid-state electrochemical reaction involving Ti^{IV} reduction in the presence of H_2O, at or near the negatively biased electrode. Whether oxygen deficiency in Ti oxide is discussed in terms of Ti^{IV} reduction or oxygen vacancies, the important factor to conductivity is the presence of electrons in the conduction band of TiO_x, which are responsible for the >8 orders of magnitude higher conductivity of TiO compared to TiO_2.[1,32] Although modulation of Ti conduction band electrons underlies the conductance changes reported for both the $Pt/TiO_2/TIO_{2-x}/Pt$ memristor and carbon/molecule/TiO_2/Au heterojunctions, the two devices differ significantly in how asymmetry is introduced into the junction interior. The memristor relies on successive layers of TiO_2 and oxygen-deficient TiO_{2-x} to create an asymmetric junction and series resistors of different magnitudes,[29,30] while in the Fl/TiO_2 device discussed here, asymmetry is introduced by the molecular layer, and doping results from electron injection into the TiO_2 from the electrode opposite to the tunneling barrier represented by the molecular layer.[31]

Following either a set pulse or exposure to H_2 or UV light, the set state of a $PPF/Fl/TiO_2/Au$ junction was more stable in the absence of O_2. Sealing a junction with glass/epoxy both prolonged the "on" state lifetime and greatly reduced the effects of humidity, consistent with the effects of water and O_2 on TiO_2 reduction. It is likely that more rigorous exclusion of O_2 by a hermetic seal would significantly prolong the lifetime of the "on" state, possibly resulting in nonvolatile memory.

The similarity of the response for junctions containing both redox active (NAB) and redox inactive (Fl and $C_{10}N$) molecules shown in Fig. 10 confirms that TiO_2 is the only redox system required to mediate the observed memory effect. As reported previously,[31] the molecular layer provides an essential tunneling barrier that permits the Fermi level to shift negative in the TiO_2 and cause reduction to Ti^{III} oxide. Fl and $C_{10}N$ have higher highest-occupied-molecular-orbital/lowest-unoccupied-molecular-orbital gaps than NAB and may provide higher tunneling barriers. The larger set currents observed for $C_{10}N$ and Fl junctions in Fig. 9 may result from their higher tunneling barriers, but this effect is modest. For $PPF/Al_2O_3/TiO_2/Au$ junctions, the alumina represents a barrier similar in height to that of $C_{10}N$, but was sufficiently thick (3.3 nm) to block dc conduction through the device.[31] These observations indicate that while a barrier is necessary to bring about TiO_2 reduction, it must be low enough to permit transmission of electrons so that the conductance change in TiO_2 accompanying reduction is observable.

Conclusions

The current results add several significant points to the previously proposed conductance switching mechanism mediated by TiO_2 redox chemistry. First, bias-induced reduction of Ti^{IV} to Ti^{III} oxide is necessary and sufficient to explain the observed conductance changes, with no requirement for identifiable redox activity in the molecular layer. Second, water is essential to the reduction process, presumably via partial hydration of Ti^{IV} oxide, although high water levels are deleterious to conductance switching. Although there is no direct evidence that water permits ion motion, it is still possible that mobile ions are involved in conductance switching. Although motion of oxygen vacancies (with +2 charge) or oxygen anions (−2) is possible, the high energy required to form these species may make ion transport by H^+ or OH^- more likely. Third, chemical reduction and oxidation with H_2 and O_2, as well as photochemical reduction by UV light produce similar changes in junction conductance to those caused by a voltage pulse, but on a slower time scale. Fourth, the observations are consistent with a mechanism involving electron injection into the TiO_2 when the bias on Au is less than −2 V, followed by a reaction of the injected electrons with hydrated Ti^{IV} sites to produce Ti^{III} oxide. The higher conductivity of Ti^{III} compared to $Ti^{IV}O_2$ produces the observed conductance increase, and this change persists until the Ti^{III} is reoxidized. Finally, the "dynamic doping" of TiO_2 responsible for the observed conductance changes in Fl/TiO_2 heterojunctions amounts to a solid-state electrochemical process, with Ti^{IV} reduction occurring at or near the negatively biased electrode. Although the detailed mechanism of the hysteresis recently associated with the memristor containing only Pt, TiO_2, and oxygen-deficient TiO_x may depend strongly on composition and fabrication, bias-induced reduction of Ti^{IV} to Ti^{III} mediated by water is at least one likely mechanism.

Acknowledgments

This work was supported primarily by the National Science Foundation through grant no. 0211693 from the Analytical and Surface Chemistry Division. Additional support in Canada was provided by NSERC, the National Research Council, and the Alberta Ingenuity Fund. The authors appreciate useful conversations with members of ZettaCore, Inc. (Denver), particularly Ken Mobley and Seth Miller.

University of Alberta assisted in meeting the publication costs of this article.

References

1. R. Waser and M. Aono, *Nature Mater.*, **6**, 833 (2007).
2. J. C. Scott and L. D. Bozano, *Adv. Mater. (Weinheim, Ger.)*, **19**, 1452 (2007).
3. C. P. Collier, J. O. Jeppesen, Y. Luo, J. Perkins, E. W. Wong, J. R. Heath, and J. F. Stoddart, *J. Am. Chem. Soc.*, **123**, 12632 (2001).
4. A. R. Pease, J. O. Jeppesen, J. F. Stoddart, Y. Luo, C. P. Collier, and J. R. Heath, *Acc. Chem. Res.*, **34**, 433 (2001).
5. E. DeIonno, H. R. Tseng, D. D. Harvey, J. F. Stoddart, and J. R. Heath, *J. Phys. Chem. B*, **110**, 7609 (2006).
6. P. Lewis, C. Inman, Y. Yao, J. Tour, J. Hutchinson, and P. Weiss, *J. Am. Chem. Soc.*, **126**, 12214 (2004).
7. P. A. Lewis, C. E. Inman, F. Maya, J. M. Tour, J. E. Hutchison, and P. S. Weiss, *J. Am. Chem. Soc.*, **127**, 17421 (2005).
8. A. M. Nowak and R. L. McCreery, *Anal. Chem.*, **76**, 1089 (2004).
9. A. Nowak and R. McCreery, *J. Am. Chem. Soc.*, **126**, 16621 (2004).
10. A. O. Solak, S. Ranganathan, T. Itoh, and R. L. McCreery, *Electrochem. Solid-State Lett.*, **5**, E43 (2002).
11. R. L. McCreery, J. Dieringer, A. O. Solak, B. Snyder, A. Nowak, W. R. McGovern, and S. DuVall, *J. Am. Chem. Soc.*, **125**, 10748 (2003).
12. S. Ssenyange, H. Yan, and R. L. McCreery, *Langmuir*, **22**, 10689 (2006).
13. M. N. Kozicki, M. Mitkova, M. Park, M. Balakrishnan, and C. Gopalan, *Superlattices Microstruct.*, **34**, 459 (2003).
14. M. N. Kozicki, M. Park, and M. Mitkova, *IEEE Trans. Nanotechnol.*, **4**, 331 (2005).
15. Q. Lai, Z. Zhu, Y. Chen, S. Patil, and F. Wudl, *Appl. Phys. Lett.*, **88**, 133515 (2006).
16. K. Sung Hoon, T. Crisp, I. Kymissis, and V. Bulovic, *Appl. Phys. Lett.*, **85**, 4666 (2004).
17. J. H. Krieger, S. V. Trubin, S. B. Vaschenko, and N. F. Yudanov, *Synth. Met.*, **122**, 199 (2001).
18. D. R. Stewart, D. A. A. Ohlberg, P. A. Beck, Y. Chen, R. S. Williams, J. O.

Jeppesen, K. A. Nielsen, and J. F. Stoddart, *Nano Lett.*, **4**, 133 (2004).
19. S.-C. Chang, Z. Li, C. N. Lau, B. Larade, and R. S. Williams, *Appl. Phys. Lett.*, **83**, 3198 (2003).
20. C. P. Collier, E. W. Wong, M. Belohradsky, F. M. Raymo, J. F. Stoddart, P. J. Kuekes, R. S. Williams, and J. R. Heath, *Science*, **285**, 391 (1999).
21. W. R. McGovern, F. Anariba, and R. McCreery, *J. Electrochem. Soc.*, **152**, E176 (2005).
22. R. McCreery, J. Dieringer, A. O. Solak, B. Snyder, A. M. Nowak, W. R. McGovern, and S. DuVall, *J. Am. Chem. Soc.*, **126**, 6200 (2004).
23. J. J. Blackstock, W. F. Stickle, C. L. Donley, D. R. Stewart, and R. S. Williams, *J. Phys. Chem. C*, **111**, 16 (2007).
24. C. A. Richter, D. R. Stewart, D. A. A. Ohlberg, and R. S. Williams, *Appl. Phys. A: Mater. Sci. Process.*, **80**, 1355 (2005).
25. R. L. McCreery, U. Viswanathan, R. P. Kalakodimi, and A. M. Nowak, *Faraday Discuss.*, **131**, 33 (2006).
26. D. S. Jeong, H. Schroeder, and R. Waser, *Electrochem. Solid-State Lett.*, **10**, G51 (2007).
27. K. Szot, W. Speier, G. Bihlmayer, and R. Waser, *Nature Mater.*, **5**, 312 (2006).
28. B. J. Choi, D. S. Jeong, S. K. Kim, C. Rohde, S. Choi, J. H. Oh, H. J. Kim, C. S. Hwang, K. Szot, R. Waser, et al., *J. Appl. Phys.*, **98**, 033715 (2005).
29. J. J. Yang, M. D. Pickett, X. Li, D. Ohlberg, D. Stewart, and R. S. Williams, *Nat. Nanotechnol.*, **3**, 429 (2008).
30. D. B. Strukov, G. S. Snider, D. R. Stewart, and R. S. Williams, *Nature (London)*, **453**, 80 (2008).
31. J. Wu, K. Mobley, and R. McCreery, *J. Chem. Phys.*, **126**, 024704 (2007).
32. R. McCreery, J. Wu, and R. J. Kalakodimi, *Phys. Chem. Chem. Phys.*, **8**, 2572 (2006).
33. R. P. Kalakodimi, A. Nowak, and R. L. McCreery, *Chem. Mater.*, **17**, 4939 (2005).
34. F. Anariba, J. Steach, and R. McCreery, *J. Phys. Chem. B*, **109**, 11163 (2005).
35. S. Ranganathan and R. L. McCreery, *Anal. Chem.*, **73**, 893 (2001).
36. S. Ranganathan, R. L. McCreery, S. M. Majji, and M. Madou, *J. Electrochem. Soc.*, **147**, 277 (2000).
37. F. Anariba, S. H. DuVall, and R. L. McCreery, *Anal. Chem.*, **75**, 3837 (2003).
38. R. S. Deinhammer, M. Ho, J. W. Anderegg, and M. D. Porter, *Langmuir*, **10**, 1306 (1994).
39. S. H. Szczepankiewicz, J. A. Moss, and M. R. Hoffmann, *J. Phys. Chem. B*, **106**, 2922 (2002).
40. S. H. Szczepankiewicz, A. J. Colussi, and M. R. Hoffmann, *J. Phys. Chem. B*, **104**, 9842 (2000).
41. M. A. Henderson, *Surf. Sci.*, **355**, 151 (1996).
42. D. A. Panayotov and J. T. Yates, *Chem. Phys. Lett.*, **410**, 11 (2005).